The buffering effect of a paper-based storage enclosure made from functional materials for preventive conservation

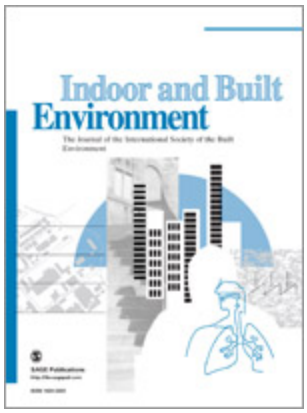

Experimental study on the buffering effect of a paper-based storage enclosure made from functional materials for preventive conservation

Journal:	*Indoor and Built Environment*
Manuscript ID	IBE-23-0127.R1
Manuscript Type:	Original Manuscript
Date Submitted by the Author:	n/a
Complete List of Authors:	Han, Bo; Heriot-Watt University, Energy Geoscience Infrastructure and Society Wang, Fan; Heriot-Watt University, Energy Geoscience Infrastructure and Society Li, Xuquan; Qingdao University of Technology, School of Environment and Municipal Engineering Bon, Julie; National Library of Scotland, Collections Care Symonds, Ian; National Library of Scotland
Keywords:	preventive conservation, enclosure, buffering capacity, material property, Hygrothermal control < Environmental Engineering
Abstract:	Storage enclosures made of paper-based materials are commonly used to store and classify archival documents for their hygrothermal buffering effect. However, there is little information about papermaking and quantitative studies on such an effect. Aiming to assess the feasibility of using the enclosure to buffer temperature and relative humidity fluctuations, without any detrimental effect on the collections, this paper reports four measurements and a feasibility assessment: thermophysical properties of the enclosure material, hygroscopic properties of the material, air change rate of the enclosure, buffering effect in a climate-chamber, and the assessment of safeguarding collections without causing any detrimental effect. The measurement results show that the enclosure can buffer macro-environmental fluctuations, which was considered sufficient to mitigate temperature and humidity fluctuations from the room environment and to secure a condition inside that is safe for the collections. The paper-based material determines the buffering capacity of the enclosure, and an appropriate air change rate ensures average temperature and relative humidity inside the enclosure at a

	controllable level and prevents off-gassing accumulation. This work provides assurance that using enclosures is an effective approach to collection storage and establishes a significant basis for further heat-air-moisture simulation and energy-saving optimization study in the service operation.

[Title page]

Experimental study on the buffering effect of a paper-based storage enclosure made from functional materials for preventive conservation

Bo Han [1], Fan Wang [1,*], Xuquan Li [2], Julie Bon [3], Ian Symonds [3]

[1] School of Energy, Geoscience, Infrastructure and Society, Heriot-Watt University, Edinburgh EH14 4AS, UK

[2] School of Environment and Municipal Engineering, Qingdao University of Technology, Qingdao 266033, China

[3] National Library of Scotland, Edinburgh EH1 1EW, UK

[*] **Corresponding Author(s):**

Fan Wang, School of Energy, Geoscience, Infrastructure and Society, Heriot-Watt University, Edinburgh EH14 4AS, UK. Email: fan.wang@hw.ac.uk

Keywords: preventive conservation; enclosure; buffering capacity; material property; hygrothermal control

Experimental study on the buffering effect of a paper-based storage enclosure made from functional materials for preventive conservation

Bo Han [1], Fan Wang [1,*], Xuquan Li [2], Julie Bon [3], Ian Symonds [3]

Abstract

Storage enclosures made of paper-based materials are commonly used to store and classify archival documents for their hygrothermal buffering effect. However, there is little information about papermaking and quantitative studies on such an effect. Aiming to assess the feasibility of using the enclosure to buffer temperature and relative humidity fluctuations, without any detrimental effect on the collections, this paper reports four measurements and a feasibility assessment: thermophysical properties of the enclosure material, hygroscopic properties of the material, air change rate of the enclosure, buffering effect in a climate chamber, and the assessment of safeguarding collections without causing any detrimental effect. The measurement results show that the enclosure is able to buffer macro-environmental fluctuations, which was considered sufficient to mitigate temperature and humidity fluctuations from the room environment and to secure a condition inside that is safe for the collections. The paper-based material determines the buffering capacity of the enclosure, and an appropriate air change rate ensures average temperature and relative humidity inside the enclosure at a controllable level and prevents off-gassing accumulation. This work provides assurance that using enclosures is an effective approach to collection storage and establishes a significant basis for further heat-air-moisture simulation and energy-saving optimization study in the service operation.

Keywords: preventive conservation; enclosure; buffering capacity; material property; hygrothermal control

[1] School of Energy, Geoscience, Infrastructure and Society, Heriot-Watt University, Edinburgh EH14 4AS, UK
[2] School of Environment and Municipal Engineering, Qingdao University of Technology, Qingdao 266033, China
[3] National Library of Scotland, Edinburgh EH1 1EW, UK

Corresponding author(s)
Fan Wang, School of Energy, Geoscience, Infrastructure and Society, Heriot-Watt University, Edinburgh EH14 4AS, UK. E-mail: fan.wang@hw.ac.uk

Introduction

The control of temperature and relative humidity (RH) is a decisive factor in preventive conservation, as it aims to maintain the environment in the right conditions to avoid possible mechanical, chemical and biological deterioration in the collections to prolong their life.[1] The consensus in the industry, to avoid detrimental effects on the collections, are: the upper limit of the room temperature is set at 25-30°C to guarantee the chemical stability of the collections and the lower one at 5°C to avoid the risk of frost damage to the building structure and condensation. The upper limit for the room RH is set at 70% to guarantee mechanical stability, and 65% (at 20°C) to reduce the risk of mould germination, and the lower one at 30% to avoid physical damage.[2, 3]

Based on the consensus, the ASHRAE (American Society of Heating, Refrigerating and Air-Conditioning Engineers) and British Standards propose standard control bands with 24-hour fluctuations for the temperature and RH control in storage spaces of museums, galleries, archives and libraries. For instance, the ASHRAE points out a level of precision control (Type A Control):10-25°C, 35%-65%RH control bands with ±2°C and ±5%-10%RH short-term fluctuations as it can minimise mould germination and mechanical damage for most paper-based artefacts. The same damage can be avoided for many artefacts and most books, except paintings and vulnerable artefacts, at the level of limited control (Type B Control): ≤30°C, 30%-70%RH control bands with ±5°C and ±10%RH short-term fluctuations.[4] The British Standard Institute suggests: 5-25°C and 30%-70%RH control bands with ±5°C and ±10%RH short-term fluctuations for general collections in BS 16893:2018. Under these specifications, the

setpoints of temperature and RH are allowed to drift to reduce energy use: 7-14°C at 30%-45%RH in winter and spring; 14-23°C at 45%-65%RH in summer and autumn.[2] For the storage of archive documents, the British Standard 4971:2017 stipulates a fixed temperature and RH setpoint within 13-16°C and 45%-60%RH with tolerances of ±1°C and ±5%RH.[5] Apart from temperature and RH, heritage collections should be monitored every six months to check for any contamination due to pollution.

Such stringent requirements for the indoor environment require precision air conditioning running continuously and consistently across a whole storage room. The use of HVAC operations, with tight environmental controls, inevitably leads to high energy consumption and carbon emissions. Additionally, in Europe, many heritage collections are housed in historic buildings that are an essential part of that cultural heritage. Finding ways to improve energy efficiency can be challenging while preserving and respecting the cultural heritage of these buildings.

As a consequence, improving the existing conditions of the structure is not always a simple task.[6] As part of a collective effort to protect both the cultural heritage and the natural environment, collections care professionals are constantly searching for innovative ways to preserve collections and energy.[7] One solution to this effort is passive environmental control, which reduces carbon emissions while ensuring environmental risk management for collections.[8]

Passive control relies on the outdoor climate moderation capability of the building structure. Buildings with a large thermal mass and hygroscopic inertia, producing airtight and thermally insulated envelopes, impede heat and mass transfer between

outdoor and indoor thus stabilising the indoor environment.[9-11] In general, the buildings which provide low energy operation for collection storage have three features for passive environmental control, "excellent combination of thermal insulation and heat capacity", "good building airtightness" and "effective absorption dehumidification".[12-14] Due to the passive environmental control, daily RH fluctuation can be stabilized at 1%-2%RH and yearly dehumidification loads decreased by 79% in a museum storage space.[15]

It is established good practice to keep that cultural collections, such as archival documents, in enclosures in order to protect them from rapid fluctuations in temperature and RH and to mitigate any malfunction of the HVAC system.[2] Because of the thermal insulation, airtightness and temperature and humidity control capacity of the enclosure, a desirable temperature and RH is achieved inside the enclosure (see Figure 1). While a relatively stable indoor temperature and RH are maintained by the air handling unit, the hygrothermal condition inside the sealed space can be further stabilised by placing inside the substances that can moderate the temperature and humidity, such as paraffin with silicon,[16] porous matrix with various hygroscopic salts,[17] composite material comprising natural polymer derivative, porous natural mineral, and acrylamide copolymer[18]. Meanwhile, the airtightness of an enclosure affects how much air flows between the enclosed space and the indoor environment. These two environments are known as the micro-environment and macro-environment, respectively. Stable temperature and RH conditions inside the showcases were maintained in a historic house whose indoor environment could not be guaranteed by

mechanical air-conditioning due to the buffering capacity of the cases with a suitable air change rate (ACR).[19]

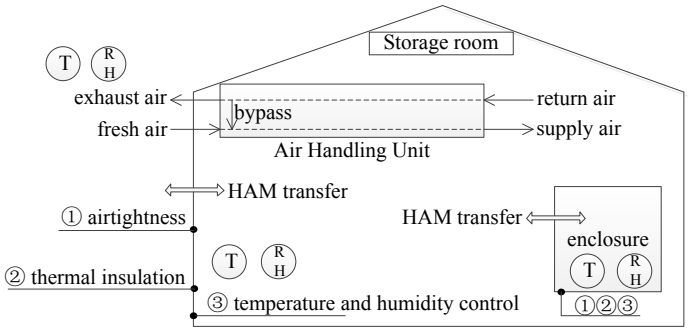

Figure 1. Schematic diagram of heat, air and moisture transfer among three elements – the outdoor, room and enclosure.

Although the capacity can increase with good airtightness, a certain degree of leakage is desirable to prevent high concentration of the off-gassing emitted from the collections inside an enclosure, which is another risk in collection care.[20] This consideration differentiates the functions of the enclosures used in storage and showcases in exhibition. A showcase is airtight to isolate the hygrothermal influence of the visitors and to protect the collections inside. The off-gassing concentration, temperature and RH are managed by a real-time micro-environment control system, involving adsorbents for pollutants and moisture removal, and active sensors.[21] This method is generally impractical for storage enclosures given the greater volume of collections in storage at most cultural institutions. Each of the enclosures relies on the ACR to maintain a satisfactory micro-environment and, together with its envelope, to mitigate the hygrothermal fluctuations and mean level. While temperature and humidity buffering in buildings is recognised, its magnitude and application within the heritage repository industry remain largely unexplored. It is uncertain how it could help cultural institutions to reduce risk the potential damage to their collection in unconditioned

space, and how it could help to achieve energy saving while maintaining quality condition for the collection using a paper-based enclosure in the passive environmental control. Hence, this study aims to assess the feasibility of using the storage enclosure to provide a buffering effect in the macro-environment control of the storage spaces. There are three objectives:

- to analyse the microstructure and hygrothermal properties of the paper-based material and test the ACR and buffering effect of the enclosure.
- to understand the nature of the buffering effect by examining the heat, air and moisture transfer of the enclosure
- to assess the feasibility of the buffering effect by deriving an acceptable threshold of buffering from a similar model test and then comparing the measured against the threshold.

The following contents were organised as Figure 2 shows.

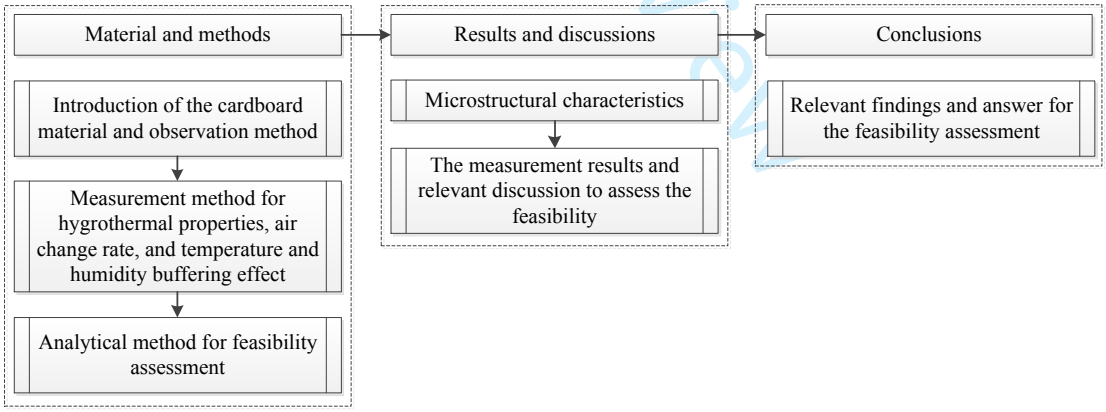

Figure 2. Contents and organization

Material and methods

Material

The storage enclosure was folded from one piece of cardboard, with full length overlays

on three-sides when it was closed (Figure 3). The cardboard was fabricated from a functional paper-based material that consists of layers of cotton pulp and polypropylene, with the addition of grounded calcium carbonate as an alkaline filler.[22] It had a thickness of 1.14mm and was composed of three tightly laminated layers that cannot be easily separated. The National Library of Scotland manufactured the enclosure using board supplied by KLUG-CONSERVATION Walter Klug GmbH & Co. KG. To create a confined micro-environment inside the enclosure, the front 230x80mm and top-bottom 180x80mm faces were made of 4-fold and 2-fold full overlaps of the cardboard and the others were uncut without any gaps. As a result, the enclosure was considered well sealed. It was tested without any contents, as the items inside might affect its buffering effect. There were two reasons: firstly, the collection items could possibly provide additional buffering capacity to mitigate the indoor fluctuations and therefore affect the actual performance of the enclosure; secondly, the collection item may stagnate the air inside the enclosure by blocking up gaps in the construction and consequently reduce the ACR (the lower ACR, the better buffering capacity). Therefore, using empty enclosures was the reasonable method for assessing the full buffering capacity of the box alone.

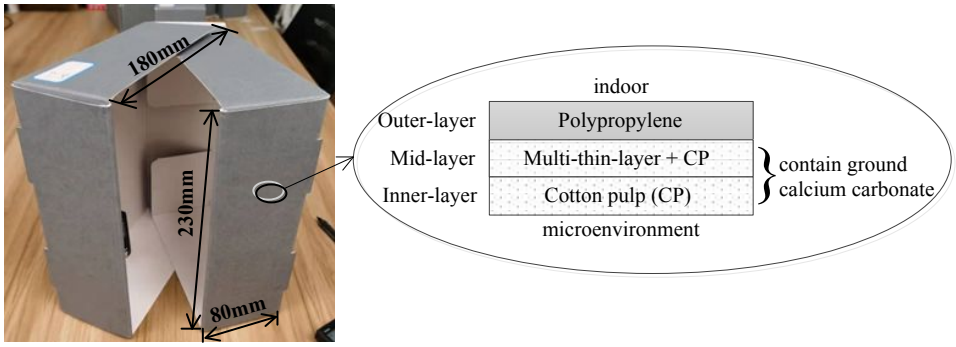

Figure 2. Enclosure sample and structure diagram of its fabric

Microstructure observation

Morphological observations of the cross section and three functional layers were conducted using scanning electron microscopy (SEM), FEI Quanta FEG 250, at an accelerating voltage of 20kV. SEM images were recorded at different magnifications: 150× for cross section, 5000× for outer-layer, 2500× for mid-layer (20,000× for locality), and 300× for inner-layer (10,000× for locality), to identify the microstructure of the cardboard.

Thermophysical property measurement

The thermal diffusivity and specific heat capacity of the material were measured at 15°C, 20°C and 25°C. The measurement was based on the laser flash method (LFM) for thermal diffusivity[23] and a comparison method with reference specimen for specific heat capacity[24], which was compliant to EN ISO 22007-4[25] and ISO 13826:2013[26]. A transient temperature change between two sides of the test specimen was recorded as a function of time and it was compared with a theoretical model to obtain the thermal diffusivity. The LFA 467 Hyper Flash, NETZSCH was used for the test. Its technical parameters are shown in Table 1. Further, thermal conductivity was calculated by Eq. 1.

$$\lambda(T) = \alpha(T) \cdot c_p(T) \cdot \rho(T) \quad (1)$$

Where λ is thermal conductivity [W/(m·K)], α is thermal diffusivity [mm²/s], c_p is specific heat [J/(g·K)], ρ is bulk density [g/cm³].

Table 1 Technical parameters for the laser flash apparatus

Technical parameter	Content
Thermal diffusivity	0.01-2000 mm^2/s
sample thickness	0.01-6 mm
Thermal conductivity	<0.1-4000 W/(m·K)
Data acquisition rate	up to 2 MHz
Accuracy	±3% for thermal diffusivity; ±5% for specific heat capacity

Hygroscopic property measurement

Equilibrium moisture content (EMC) is used to indicate the ratio of the mass of moisture content inside the material to the mass of the specimen with zero moisture content. An EMC curve can describe moisture gains and losses for hygroscopic materials in various temperature and RH. Water vapour diffusion resistance coefficient and water vapour diffusion coefficient are critical indicators to indicate water vapour permeability through the material.[27] Three measurements based on the weighting method are introduced as follows. Technical parameters of the testing instrument are shown in Table 4.

Measurement for EMC curves. Measurement of EMC was in accordance with BS EN ISO 12570:2000+A2:2018 [28] and BS EN ISO 12571:2013.[29] The weight difference was measured between the equilibrium state and the dry state at a specific temperature and relative humidity to determine the moisture content. The tested range of temperature and RH was set at 15-25°C and 30%-70%RH due to a common range of control bands in the standards. Table 2 shows the equilibrium conditions. RH is maintained by saturated solution in a sealed desiccator while the enclosure is stored in a constant temperature chamber.

Table 2 Air relative humidities above saturated solutions in equilibrium (Unit: %RH)

Temperature	$MgCl_2$	K_2CO_3	NaBr	NaCl
15°C	33.30±0.21	43.15±0.33	59.14±0.44	75.61±0.18
20°C	33.07±0.18	43.16±0.33	58.20±0.42	75.47±0.14
25°C	33.78±0.16	43.16±0.39	56.95±0.39	75.29±0.12

Measurement for water vapour diffusion resistance coefficient. The water vapour diffusion resistance coefficient was obtained by testing water vapour permeability, according to BS EN 15803:2009.[30] The test specimen was mounted in a cup with specific RH inside, which was kept in a chamber with fixed RH to create different partial water vapour pressures on two sides of the specimen. The change in mass was measured at 24-hour intervals to determine the permeability of specimens under two test conditions. The first one was low-humidity conditions, with the micro-environment and macro-environment stabilized at 0-3%RH and 50%RH, respectively. Moisture transfer occurred from the outside of the enclosure to the inside. The second one was high-humidity conditions, with the micro-environment and macro-environment stabilized at approx. 93%RH and 50%RH, respectively. Moisture transfer occurred from the inside of the enclosure to the outside. Silica gel and $NH_4H_2PO_4$ were used as humidity-control materials. Both tests were conducted at 20°C. The chamber's built-in temperature and humidity sensor monitored the macro-environment.

Water vapour diffusion resistance coefficient, μ, is a function of using water vapour permeability of air (δ_a) versus water vapour permeability (δ_p), $\mu = \delta_a/\delta_p$. Water vapour permeability of air is defined by the Schirmer equation (Eq. 2).[31]

$$\delta_a = 0.0000231 \times \frac{p_0}{p \times R \times T} \times \left(\frac{T}{273}\right)^{1.81} \quad (2)$$

Where p_0 is standard barometric pressure [Pa]; p is barometric pressure [Pa]; T is temperature in the chamber [K]; R is gas constant for water vapour [Nm/(kg·K)].

Cumulative mass change, Δm_i, is calculated by Eq. 3.

$$|\Delta m_i| = m_i - m_0 \quad (3)$$

Where m_i and m_0 are the mass of test assembly respectively at time t_i and t_0.

Water vapour flow rate, G [g/s], is calculated by Eq. 4.

$$G = \frac{\Delta m}{\Delta t} \quad (4)$$

Water vapour permeance, W_p, is given by Eq. 5.

$$W_p = \frac{G}{A \cdot \Delta p_v} \quad (5)$$

Where A is test surface area (7.07cm^2); Δp_v is calculated from the temperature and RH of test conditions. Water vapour permeability is calculated by Eq. 6, $\delta_p = W_p \cdot D$ (D is thickness of the specimen).

Measurement for water vapour diffusion coefficient. Water vapour diffusion coefficient is subject to water vapour concentration gradients. Its measurement method is based on ASTM E96-00E1.[32] Successive weightings at an interval of 24h were carried out to record the mass change in the specific gradients and further calculate the diffusion coefficient. Table 3 shows the test conditions within 15-20°C and 33%-75%RH. The sample was treated as a single integrated layer block during measurement because the construction of the cardboard meant it was challenging to measure the three individual layers separately.

Table 3 Test conditions for water vapour diffusion

	cup RH	cup and chamber temperature	chamber RH	RH difference
NaCl	75.47%±0.14%RH	20 ±0.5°C	45%±2.5%RH	-30%RH
NaCl	75.47%±0.14%RH	20 ±0.5°C	55%±2.5%RH	-20%RH
NaCl	75.47%±0.14%RH	20 ±0.5°C	65%±2.5%RH	-10%RH
NaCl	75.47%±0.14%RH	20 ±0.5°C	70%±2.5%RH	-5%RH

According to Fick's first law[33], diffusion coefficient, D_W, can be described by

using diffusive flux of water vapour over the concentration gradient (Eq. 7).

$$D_W = \frac{M_W/tA}{\Delta C/L} \quad (7)$$

Where M_W is mass of water vapour through the specimen for time t [g]; t is time in water vapour diffusion [s]; A is surface area [m^2]; L is thickness of specimen in the diffusion direction [m]; ΔC is concentration difference of water vapour [g/m^3]. ΔC can be described by the difference of moisture content between the surfaces of the specimen (Eq. 8).[34, 35]

$$\Delta C = \Delta u \cdot SG \cdot \rho_w \quad (8)$$

Where ρ_w is density of water [kg/m^3]; SG is specific gravity of the specimen in specific moisture content, $SG = \rho_{specimen}/\rho_w$, $\rho_{specimen}$=662 kg/m^3; Δu is the difference of moisture content between upper and lower surfaces of the specimen and it can be obtained by the EMC curves, $u = f(T,RH)$.

Table 4 Technical parameters of balance and constant temperature chamber

Testing instrument	Technical parameter	Content
SATORIUS analytical balance	Maximum capacity	220g
	Scale interval	0.1mg
Minquan MQL-61R constant temperature chamber	Temperature control range	4-60℃
	Temperature accuracy	±0.1℃
	Temperature uniformity	±0.5℃at37℃

Air change rate of an enclosure

The tracer gas decay method using CO_2 aims at cumulatively assessing the air and gas tightness of the envelope.[8] CO_2 was selected as the tracer gas because its density is similar to air, which consequently can simulate similar behaviour of air exchange.[36] The measurement followed ASTM E741-11.[37] A small volume of tracer gas (<5000ppm) was released into the enclosure, and then the concentration was recorded

at a 5-second interval. The measured data was fitted into the following custom equation (Eq.9) to obtain the ACR value.

$$C(t) = C_0 e^{-\frac{Q_{ex}}{V_e}t} \quad (9)$$

Where $C(t)$ is CO_2 concentration at the sampling time [ppm]; C_0 is the CO_2 concentration at the beginning [ppm]; t is time [s]; Q_{ex} is air exchange volume and V_e is the enclosure volume and $\frac{Q_{ex}}{V_e} = ACH$.

The air movement was kept minimal (<0.5m/s) in the laboratory, similar to real practice in the storage room.[38] The ACR was obtained by regression calculation of the decay curves. Relevant technical parameters of air quality meter and anemometer are shown as following table 5.

Table 5 Technical parameters of air quality meter and anemometer

Testing instrument	Technical parameter	Content
TSI indoor air quality meter IAQ-CALA7545 (CO_2)	Range	0 to 5000 ppm
	Accuracy	±3% of reading or ±50 ppm, whichever is greater
	Resolution	1 ppm
TESTO 417 anemometer	Range	0.3 to 20 m/s
	Accuracy	±0.1m/s
	Resolution	0.01m/s

Temperature and humidity buffering effect of the enclosure

A similar simulation test was used to simulate the macro-environment fluctuations.[39] Test amplitudes of the macro-environment fluctuations were based on the maximum, 5°C and 10%RH for 24-hour fluctuations and 17-22°C and 50%-60%RH for control bands in relevant standards.[2-4] Fluctuation periods were designed according to a consideration of steady state of heat and mass transfer between micro-environment and macro-environment. Table 6 shows six independent test conditions. All fluctuations are harmonic oscillation.

There was a 24h acclimatization process at the initial conditions (17°C at 50%RH and 50%RH at 20°C) to control the initial moisture content inside the material before the test. Air velocity was kept at <0.5m/s in the chamber to ensure the same condition for air exchange as in the ACR measurement. A schematic diagram of measurement apparatus is shown in Figure 4. A programmable test chamber generated macro-environment temperature and RH fluctuations with designated fluctuation periods. Two temperature and humidity loggers were set inside the chamber and enclosure, respectively. Table 7 shows their technical parameters. There were no other contents (buffer materials) inside the enclosure.

Two types of indicators were defined to quantify how much of the buffering effect

was created at a given macro-environment fluctuation. The first is the absolute reduction of fluctuation, respectively for temperature buffering (TB) [°C] and humidity buffering (HB) [%RH]:

$$TB = \Delta T_{ma} - \Delta T_{mi} \tag{10}$$

$$HB = \Delta RH_{ma} - \Delta RH_{mi} \tag{11}$$

The second is the relative ratio of the amplitude of micro-environment over that of the macro-environment. Again respectively, for the temperature fluctuation (AR_T) and RH fluctuation (AR_{RH}):

$$AR_T = \frac{\Delta T_{mi}}{\Delta T_{ma}} \tag{12}$$

$$AR_{RH} = \frac{\Delta RH_{mi}}{\Delta RH_{ma}} \tag{13}$$

Subscript ma is for the macro-environment and mi is for the micro-environment.

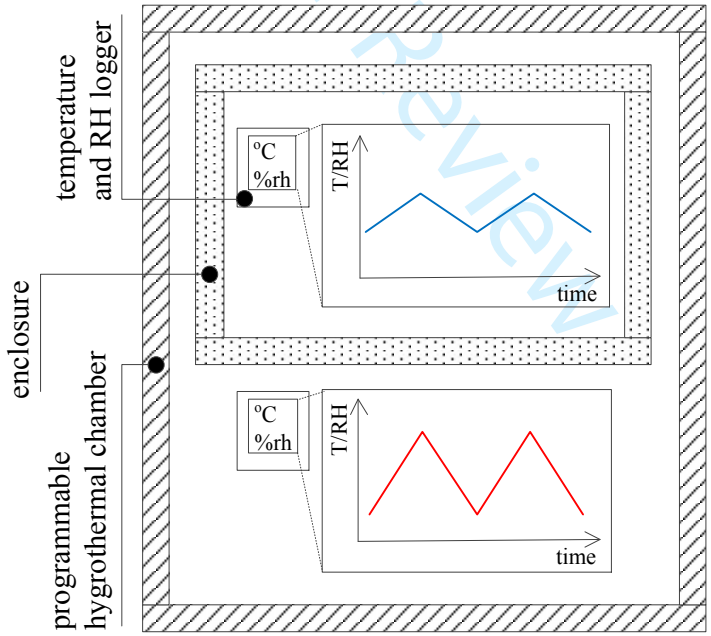

Figure 4. Schematic diagram of the measurement apparatus for buffering effect test

Table 6 Test conditions of buffering effect in temperature and RH

No.	period of fluctuations	T and RH fluctuations in the chamber	illustration of harmonic oscillation
T1	60min	17-22°C at fixed 50%RH	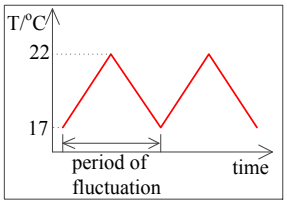
T2	120min		
T3	180min		
RH1	60min	50%-60%RH at fixed 20°C	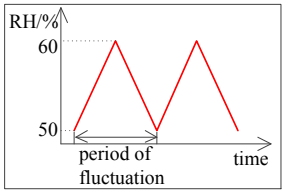
RH2	240min		
RH3	600min		

Table 7 Technical parameters of test chamber and logger

Testing instrument	Technical parameter	Content
TERCHY HRMB-120R test chamber	Range	-20 to 100℃; 30 to 95%RH
	Accuracy	±0.5℃; ±2.5%RH
	Uniformity	±1℃; ±3%RH
TESTO 174H temperature and humidity logger	Range	-20 to 70℃; 0 to 100%RH
	Accuracy	±0.5℃; ±3%RH
	Resolution	0.1℃; 0.1%RH

Feasibility analysis of using the enclosure

The enclosure in a storage room was a 'room in room' condition, for which the inner room of protection worked against the macro-environment fluctuation. Compared with unpackaged storage, using the enclosure provided a stable hygrothermal environment to avoid physical damage. However, it is important to ensure that the micro-environment within the enclosure is easy to control, as the enclosure could potentially cause chemical damage if it behaves like a greenhouse and concentrates off-gassing accumulations.[40] Hence, there were two factors to be considered in the feasibility analysis: the ACR for diluting high-concentration off-gassing and the buffering capacity for moderating an aggressive macro-environment.

The precondition for utilizing the enclosure was the implementation of an

appropriate ACR to prevent the chemical damage associated with the greenhouse issue and high-concentration off-gassing accumulations. In addition, it was necessary to quantify the buffering capacity and calculate the duration of its effectiveness to accurately evaluate the benefits. In detail, there are three parts of the feasibility analysis: firstly, to assess the greenhouse problem by comparing mean values of temperature and RH in the micro-environment with the ones in the macro-environment; secondly, to assess the off-gassing problem based on conservators' experience; thirdly, to analyse one collection-year macro-environment data of on-site monitoring in a typical collection storage scenario with 1-hour fluctuations. The analysis of 1-hour fluctuations revealed that the buffering effect persisted when the on-site fluctuations exceeded 5°C and 10%RH. Therefore, any fluctuations equal to or greater than 5°C and 10%RH were deemed indicative of the existence of a buffering effect. Furthermore, the total duration of the buffering effect was summed up to quantify its benefits.

Results and discussions

Microstructure of the material

The scanning electron microscopy (SEM) images taken as the first step in the study (Figure 5) reveal the three-layer structure made of meshes of fibres and voids. The size of the voids increases from the outer-layer (1-5μm) to the mid-layer (4-10μm) and inner-layer (5-15μm). In the outer-layer, polypropylene is fused into the fibre surface, which creates hydrophobic properties and low water vapour permeability to avoid water damage from the ambient environment.[41] In the next two layers, cotton pulp, allowing spherical calcium carbonate particles to attach the fibre structure, turns them into

thermal insulation layers.[42] The diameter of the particles is about 2μm. The mid-layer is overlaid by multiple extra-fine membranes to increase the tortuosity of the micro-porous channels. The porous structure with grounded calcium carbonate regulates the uptake and retention of moisture.[43] Moreover, the small gaps between the membranes also increase vapour retention to enhance the moisture buffering capacity.[44] The inner-layer is one single mesh of cotton fibres. Apart from the voids in the mesh, the fibres have oval pores. These pores are about 1μm on the short axis and 2μm on the long axis. Both the voids and pores form micro-passages that makes vapour transfer easier here than in the mid-layer, thus decreasing the response time of moisture absorption and desorption. The microstructure of the specially fabricated paper is the key in regulating the heat and mass transfer through the enclosure.

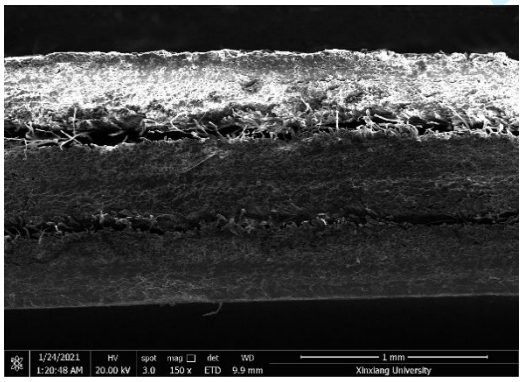

the cross-section

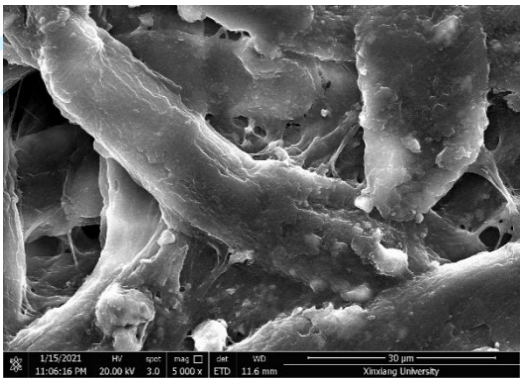

the outer-layer

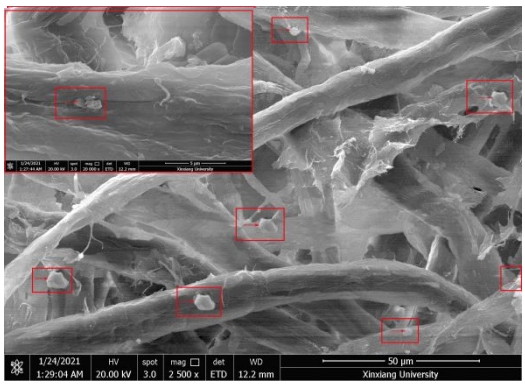

the mid - layer

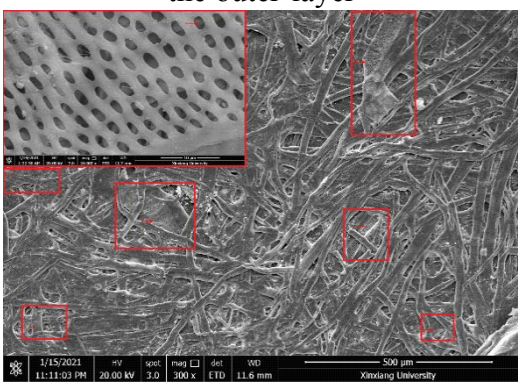

the inner-layer

Figure 5. SEM images of the material

Figure 6 illustrates three functional layers of the material. The outer-layer provides low water vapour permeability to repel water vapour from passing through the tiny voids on the external surface. The mid-layer is a barrier stopping heat/cold from conducting through the material. The inner-layer is an excellent moisture absorbent to absorb "sweat" inside the enclosure. Simultaneously, the "sweat" can be seeped to the macro-environment because the size distribution of the gaps in the fabric structure creates the driving force of water vapour concentration gradient. Depending on the appropriate ACR, coupling between passive control (hydrothermal behaviour of the enclosure) and boundary control (the macro-environment control)[45] creates the buffering effect required for safe collection storage.

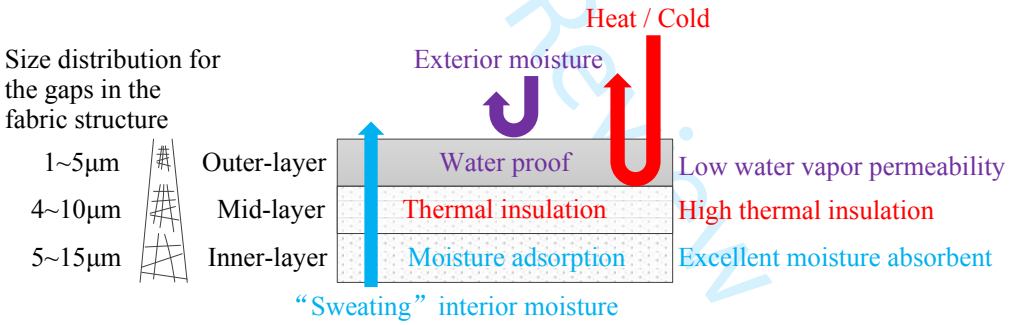

Figure 6. Functional structure of the material

Thermal properties of the material

Table 8 shows the thermal diffusivity, specific heat capacity and thermal conductivity at 15°C, 20°C and 25°C. The value of thermal diffusivity lies in 0.081-0.083mm^2/s and the value of specific heat capacity lies in 1.01-1.053J/(g·K). Thermal conductivity is varied in 0.055-0.056W/(m·K) ($\lambda = \alpha \cdot c_p \cdot \rho$, ρ=0.662g/cm^3). Compared with the thermal conductivity of substantial insulating materials (0.02-0.06 W/(m·K) at 10°C)

that are measured in the BRE Scottish Laboratory[46], the paper-based material actually plays a thermal insulation role. Moreover, its high specific heat capacity and thermal diffusivity lead to short-term thermal storage, which can effectively manage peaks and troughs of indoor thermal load fluctuations by absorbing and releasing heat from the air. These attributes make it a viable option for thermal energy storage. [47]

Table 8 Thermophysical parameters of the material

	Thermal diffusivity [mm^2/s]	Specific heat capacity [J/(g·K)]	Thermal conductivity [W/(m·K)]
15°C	0.083	1.010	0.055
20°C	0.082	1.022	0.055
25°C	0.081	1.053	0.056

Note: the thermal diffusivity and specific heat capacity are obtained from the LFA directly and thermal conductivity is calculated by using Eq. 1.

Hygroscopic properties of the material

EMC. Figure 7 shows the measurement results of EMC (Equilibrium moisture content) curves. The curves are almost linear, which suggests that they are categorized to the linear middle section of reversible type II in major physisorption isotherms without hysteresis loop for moisture adsorption and desorption. This physical process occurs when monolayer coverage completes, and capillary condensation begins.[48] The linear correlation between EMC and RH suggests that the mass of moisture content absorbed or released from the material is constant in each degree of RH fluctuation (ΔEMC/ΔRH = approx. 0.12). This constant capacity of regulating moisture from the surrounding air helps to control a stable absolute humidity (AH) in the micro-environment. AH drops can produce shrinkage of the collection materials due to moisture desorption, conversely, AH rises can produce expansion of materials due to moisture adsorption.[49]

Comparing the EMC in different temperatures, the EMC at low temperature is greater than that at high temperature. Moisture retention of the material is slightly better at low temperature than at high temperature. EMC range is 0.048-0.080g/g in 15-25°C and 40%-60%RH. Ideally, the maximum release or absorption of moisture can reach 3.586g to regulate the micro-environment humidity in a complex process of moisture transfer.[50]

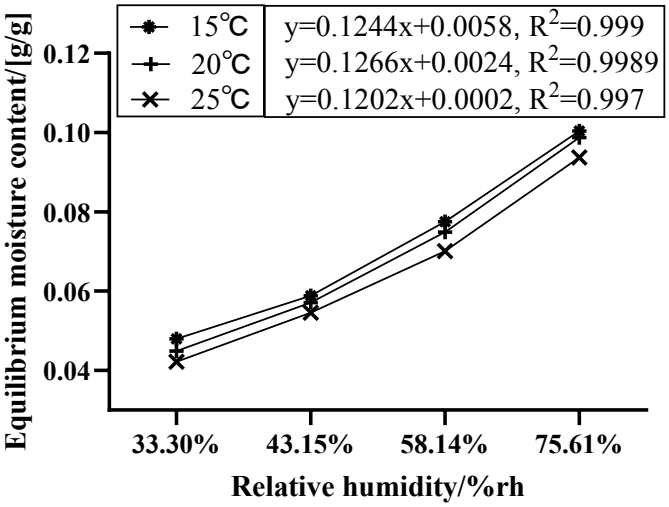

Figure 7. Equilibrium moisture content in different temperature

Water vapour diffusion resistance coefficient. For the water vapour flux through the specimen at low (silica gel, 3%→50%RH, micro-environment → macro-environment) and high ($NH_4H_2PO_4$, 93%→50%RH, micro-environment → macro-environment) humidity levels at 20°C, Table 9 shows the mass changes in the final six aligned points and Table 10 shows the calculation results. The water vapour diffusion resistance coefficients are 144.48 and 46.78 at low and high humidity levels, respectively. This feature of higher resistance to inwards diffusion makes it easy to maintain a stable RH inside the enclosure against the fluctuation in the room. The easy outward diffusion can also avoid the RH increasing when the contents accidentally retain a trace of vapour that is higher than normal.

Table 9 The mass change in the final six aligned points (unit: mg)

Time/h	0	24	48	72	96	120	Fitting function	R^2
Silica gel/g	194.7734	194.8772	194.9806	195.0776	195.1775	195.2745	y=0.004171x+194.8	0.9998
$NH_4H_2PO_4$/g	214.1814	214.9063	214.6268	214.363	214.0852	213.8081	y=-0.01142x+215.2	0.9999

Note: the water vapour flow rates (Eq.4: $G = \Delta m/\Delta t$) were calculated by the fitting function. It is 0.004171mg/h (1.15856E-09kg/s) in low humidity condition and it is

0.01142mg/h (3.17245E-09kg/s) in high humidity condition.

Table 10 Calculation of water vapour (wv) diffusion resistance coefficient

parameter	basis of calculation	results
wv flow rate, G	Eq. 4	1.15856E-09kg/s (silica) 3.17245E-09kg/s ($NH_4H_2PO_4$)
wv pressure difference across the specimen, Δp_v	psychrometric chart	1363.0Pa (s) 1208.5Pa (N)
wv permeance per Pa, W_p	Eq. 5	1.20255E-09kg/(m² · s · Pa) (s) 3.71389E-09kg/(m² · s · Pa) (N)
wv permeability, δ_p	Eq. 6	1.37091E-12kg/(m · s · Pa) (s) 4.23383E-12kg/(m · s · Pa) (N)
wv permeability of air, δ_a	Eq. 2	1.98064E-10kg/(m · s · Pa) (s) 1.98064E-10kg/(m · s · Pa) (N)
wv diffusion resistance coefficient, μ	$\mu = \delta_a/\delta_p$	144.48 (s) 46.78 (N)

Water vapour diffusion coefficient. Table 11 shows the calculation results in tested gradients from macro-environment to micro-environment. The diffusion coefficients lie in 1.38E-10 to 1.59E-10 m^2/s. There is a positive correlation between RH gradient and diffusion coefficient. Compared with the diffusion coefficient for water vapour in air at 20°C, 2.242E-5 m2/s,[51] the paper-based material of the enclosure obviously hinders the water vapour in diffusive transport.

Table 11 Calculation of water vapour diffusion coefficient

parameter	basis of calculation	results
difference of moisture content between two surfaces of the specimen, Δu	EMC curve	0.00633g (5%ΔRH) 0.01266g (10%ΔRH) 0.02532g (20%ΔRH) 0.035448g (30%ΔRH)
concentration difference, ΔC	Eq. 8	4190.46g/m^3 (5%ΔRH) 8380.92g/m^3 (10%ΔRH) 16761.84g/m^3 (20%ΔRH) 23466.58g/m^3 (30%ΔRH)
mass of water vapour through the specimen, M_W	Weight change of the specimen in equilibrium state	0.0311g (5%ΔRH) 0.0636g (10%ΔRH) 0.1367g (20%ΔRH) 0.1996g (30%ΔRH)
water vapour diffusion coefficient, D_W	Eq. 7	1.38E-10m^2/s (5%ΔRH) 1.42E-10m^2/s (10%ΔRH) 1.52E-10m^2/s (20%ΔRH) 1.59E-10m^2/s (30%ΔRH)

Note: interpolation was used to search moisture content for the points which are not on the EMC curves (Figure 7).

Air change rate of the enclosure

Figure 8 shows the concentration decay curves (background CO_2 has been deducted). By fitting the measured decay curve into the custom format of the Eq.9 (R^2= 0.9998), 19.5 air changes per hour (ACH) was obtained. This suggests that, theoretically, all air in the micro-environment can be replaced with the air in macro-environment for approx. 185 seconds.

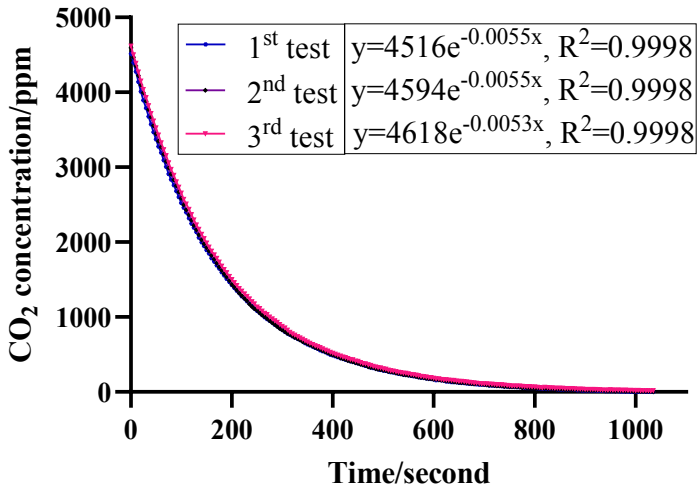

Figure 8. CO_2 concentration decay inside the enclosure

The ACR (Air change rate) of this enclosure appears to be very high when compared to display showcases.[52, 53] However, this difference can be attributed to the fact that the showcases were tightly sealed to isolate their micro-environment from the macro-environment, including the hygrothermal conditions of the exhibition areas that visitors can affect. Additionally, the micro-environment in each showcase was actively monitored and controlled by a mini air-conditioning device inside. In contrast, the enclosure discussed here was used in a storage room where visitors' behaviour does not impact the hygrothermal conditions. Furthermore, it needs to be breathable to dilute the concentration of off-gassing released by the collections. This practice is necessary in collection care, and a relatively high ACR is considered normal, even though no assessment has been conducted to determine a specific ACR that would prevent pollution-related damage.

It would be interesting to find the acceptable ACR based on the upper limit of the off-gassing concentration to safeguard the collections. But the limit is considered on a case-by-case basis due to complex chemical reactions in various collections materials.[54,

[55] The previous observation did not find noticeable chemical damage among the collections stored in such type of enclosures over years. Hence, we accepted the current level of ACR in the enclosures in testing the buffering effect.

Temperature and humidity buffering effect of the enclosure

Figure 9 shows recorded temperature and RH fluctuations. The results demonstrate that micro-environment fluctuations are 1-2°C and 2%-8%RH smaller than macro-environment ones with approximate 2-7min (temperature) and 4-9min (RH) time lags. By increasing the fluctuation period, temperature and RH differences between micro-environment and macro-environment are decreased until heat and mass transfer reach a relatively steady state. The differences are <0.5°C and <1%RH when their fluctuation periods are longer than 180min and 600min, respectively. Considering the measurement errors, the buffering effect was detected in 5°C fluctuations at 17-22°C and fixed 50%RH during <180min period and 10%RH fluctuations at 50%-60%RH and fixed 20°C during <600min period in the similar simulation test.

Figure 10 shows the quantitative results: the values of TB (temperature buffering) and AR_T are 2°C and 0.6, 1.6°C and 0.68, 1°C and 0.8 for ↑↓5°C macro-environment fluctuation during 60, 120 and 180min periods at fixed 50%RH; the values of HB (humidity buffering) and AR_{RH} are 8%RH and 0.2, 6%RH and 0.4, 2%RH and 0.8 for ↑↓10%RH macro-environment fluctuation during 60, 240 and 600min periods at fixed 20°C. The time lags between their extremums are 2-7min for temperature fluctuations and 4-9min for humidity fluctuations. These quantitative results prove that a degree of buffering can be created by using the enclosure for short-term macro-environment

fluctuations. Due to pure curiosity, a few extra tests were carried out for the enclosures with some paper-based collections. The results showed increased buffering capacity. This supports our earlier assumptions.

Maximum deviations of average temperature and RH between the micro-environment and macro-environment are 0.2°C and 1%RH. This suggests that the average temperature and RH in the micro-environment can follow the macro-environment while the fluctuations are mitigated. Hence, the greenhouse problem can be avoided. The desired micro-environment can be maintained without the need for any additional real-time monitoring solutions inside the enclosure.

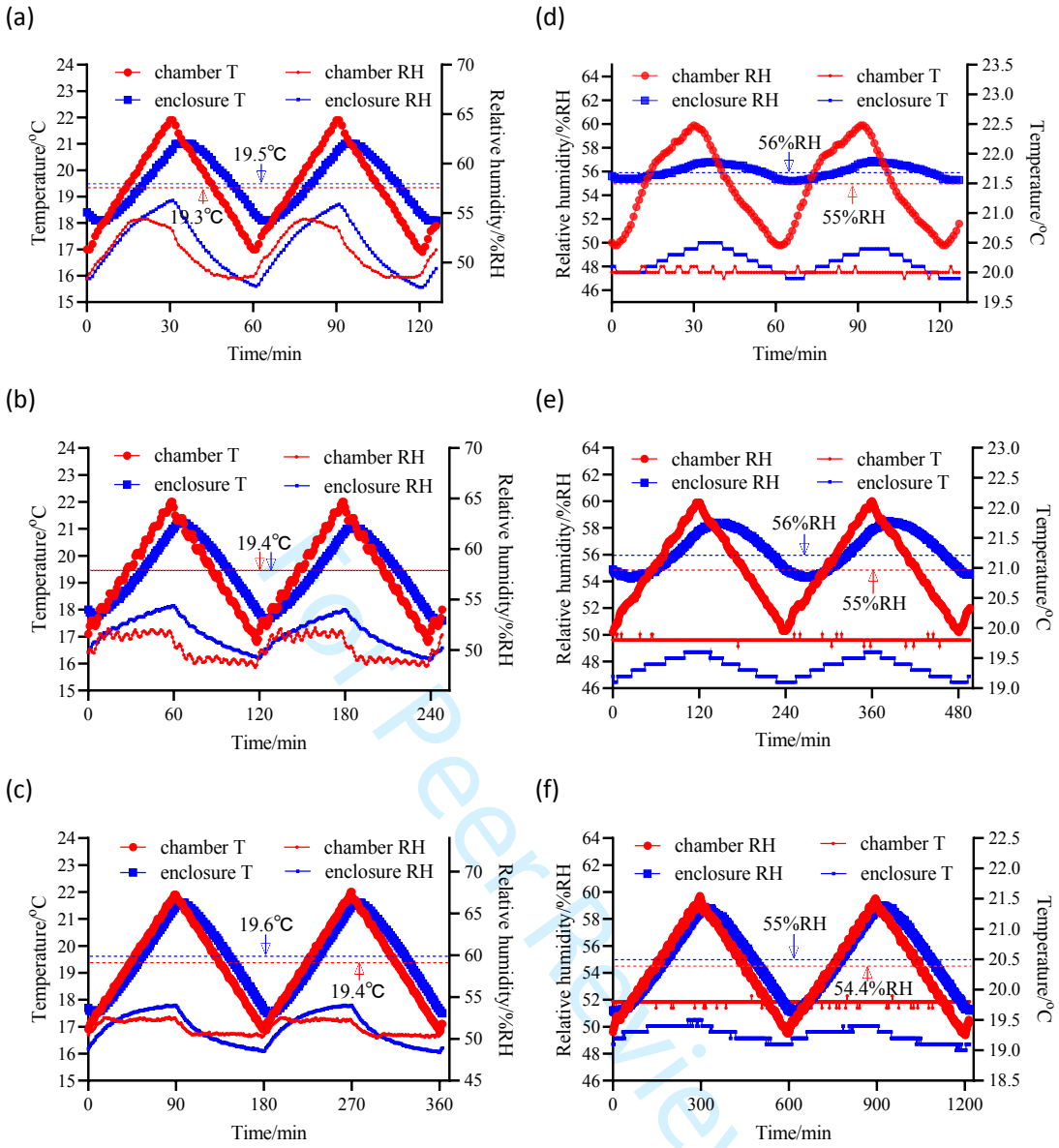

Figure 9. Temperature and RH in the chamber and enclosure (a) No. T1 60min-period; (b) No. T2 120min-period; (c) No. T3 180min-period; (d) No. RH1 60min-period; (e) No. RH2 240min-period; (f) No. RH3 600min-period

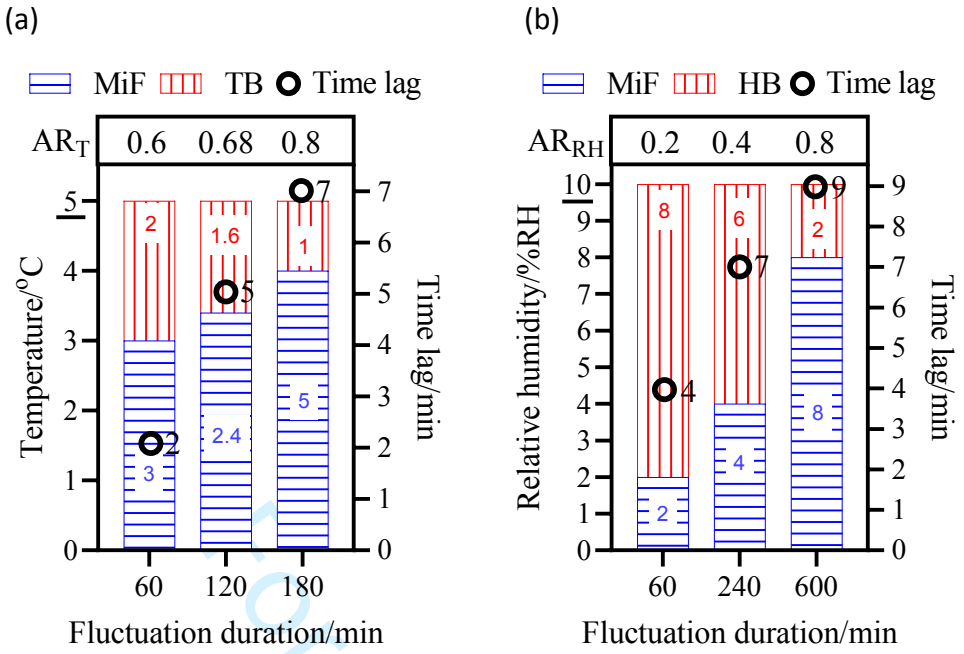

Figure 10. Quantitative indicators for buffering effect (a) temperature buffering; (b) humidity buffering

Note: MiF is Micro-environment fluctuation; Macro-environment fluctuations (MaF) are fixed at 5℃ for TB test and 10%RH for HB test; time lag is time between the peaks/troughs of MiF and MaF.

To assess the feasibility of using the enclosure, the frequency analysis of hourly temperature and RH fluctuations in a storage room with limited control was conducted. Table 12 shows the distribution of temperature and RH fluctuations for a whole year. Based on 2°C *TB* (0.6 AR_T) and 4%RH *HB* (0.2 AR_{RH}) during 1h fluctuation periods in the test conditions, the abnormal conditions such as the malfunction of an air conditioning system over allowable temperature and RH fluctuations (5°C and 10%RH) can be avoided for 0.06% and 2.2% period, respectively. The extreme RH fluctuations can be reduced for 0.3% period. The details are shown in Table 5, which indicates that the enclosure can provide buffering capacity for 219h (RH) and 53h (temperature) in the collection year. It can avoid the high risk of sudden mechanical damage such as delamination and deformation to most artifacts and paintings.[3] Given this identified

buffering capacity, the enclosure would be able to mitigate the short-term temperature and humidity fluctuations in an unconditioned room. However, the actual effectiveness of this depends on the local climate and building performance.

The buffering capacity can provide more a stable micro-environment for preventive conservation when the macro-environment temperature and RH are within the allowable fluctuations. If we focus on the micro-environment rather than the macro-environment for environmental regulation, the tight control of the macro-environment can be relaxed for energy saving in theory.

Table 12. Data distribution of room environment fluctuations in 1h period

Temperature fluctuation/^{o}C	Frequency/year^{-1}	Percentage
$0 < \Delta T \leq 5$	8778	99.94%
$5 < \Delta T \leq 6.1$	5	0.06%
RH fluctuation/ %RH	Frequency/year^{-1}	Percentage
$0 < \Delta RH \leq 10$	8563	97.5%
$10 < \Delta RH \leq 18$	197	2.2%
$18 < \Delta RH$	23	0.3%

However, we recognize that our study has the following limitations:

1) There is a lack of scientific assessment for off-gassing accumulation levels in this ACR. However, measurement of this is the beyond the scope of this research because the pollutant interactions are too complicated to quantify and manage even in the field of preventive conservation.

2) The frequency analysis of in-site temperature and RH fluctuations focuses on hourly fluctuations only. The main reason for this is how the setting of sampling intervals in the BMS (Building Management System) need to be done. In this instance it was pre-set and if fixed at 15min. 30min and 45min fluctuations are quite small when they were compared with the accuracy of the temperature and humidity logger.

3) The minimum duration is also one hour in the similar simulation test. The shorter duration should be considered for further study when there is a sufficiently accurate climate chamber for this work.

4) Because of the limitation of chamber control for de-coupling temperature and RH, the fixed parameters cannot be stabilized at the setpoint. Comparing fluctuations of the fixed parameter between micro-environment and macro-environment, there is an unexplainable phenomenon: the micro-environment fluctuations were slightly greater than the macro-environment ones. This phenomenon may relate to some complex reactions inside the material, but it should be studied further.

5) It is difficult to conduct a standardized and long-term assessment of the enclosure's life-cycle performance due to the unique usage patterns and random usage frequency. In practice, if an enclosure shows signs of appearance deformation, it is typically replaced with a new one.

Conclusions

A storage enclosure made from functional paper-based materials was investigated to assess its feasibility in collection storage. Four kinds of property measurements (thermophysical property, hygroscopic property, ACR and buffering effect of temperature and RH) were conducted and two aspects of contents, safeguarding and buffering capacity, were analysed. The following conclusions were derived:

1) Using the storage enclosure can achieve an improvement of the micro-environment without the environmental risks caused by undesirable temperature and

RH fluctuations, greenhouse problems and off-gassing concentration.

2) The properties of the paper-based material were essential in providing a buffering effect with waterproofing and thermal insulation. An appropriate ACR helped to dilute the off-gassing concentration and regulate the average temperature and relative humidity within the enclosure for collection care purposes.

3) Two types of indicators, absolute reduction of fluctuation and relative ratio of the amplitude, were proposed to quantify the buffering capacity.

4) It is feasible to use the enclosure to mitigate short-term temperature and RH fluctuations of the macro-environment in the storage room.

This study has a great significance for evaluating the buffering capacity of the enclosure and gives us an assurance to continue boxing our collections in storage as a common practice. With paper-based collections inside the enclosures, the buffering effects would be stronger. In addition, it provides boundary conditions for further numerical simulation study of heat, air and moisture transfer between micro-environment and macro-environment, which might open up an opportunity to relax environmental controls and consequently reduce the energy use in the service operation.

Acknowledgement

This work is a part of three-year PhD study, funded by the Energy Technology Partnership, Scotland (ETP 173 - 2019)

Declaration of Conflicting Interests

The author(s) declared no potential conflicts of interest with respect to the research, authorship, and/or publication of this article.

Funding

The author(s) received no financial support for the research, authorship, and/or publication of this article.

ORCID iDs

Bo Han https://orcid.org/0009-0003-1464-2135
Fan Wang https://orcid.org/0000-0003-0020-1470

Note

Author contributions	BH: Methodology, Data acquiring & analysing, Writing - original draft, Writing – review & editing. FW: Conceptualisation, Methodology, Writing – review & editing, Supervision. XQL: Methodology, Resources, Supervision. JB: Conceptualisation, Writing – review & editing. IS: Conceptualisation. All authors have read and agreed to the published version of the manuscript.

References

1. Erhardt D and Mecklenburg M. Relative humidity re-examined. *Studies in conservation* 1994; 39: 32-38.
2. Institution BS. *Conservation of Cultural Heritage: Specifications for Location, Construction and Modification of Buildings Or Rooms Intended for the Storage Or Use of Heritage Collections*. BSI Standards Limited, 2018.
3. Sharif-Askari H and Abu-Hijleh B. Review of museums' indoor environment conditions studies and guidelines and their impact on the museums' artifacts and energy consumption. *Building and Environment* 2018; 143: 186-195.
4. Sharp TR. *2019 ASHRAE Handbook: HVAC Applications-Chapter 37-Energy Use and Management*. 2020. Oak Ridge National Lab.(ORNL), Oak Ridge, TN (United States).
5. Institute BS. Conservation and care of archive and library collections, BS 4917: 2017. 2017.
6. Harrestrup M and Svendsen S. Internal insulation applied in heritage multi-storey buildings with wooden beams embedded in solid masonry brick façades. *Building and environment* 2016; 99: 59-72.
7. Lee SS. An Interview with Roderick Whitfield on the Stein Collection in the British Museum. *The Silk Road* 2019; 17: 10-25.
8. Bickersteth J. IIC and ICOM-CC 2014 Declaration on environmental guidelines. *Studies in Conservation* 2016; 61: 12-17.
9. Padfield T and Larsen PK. Low energy air-conditioning of archives. *Journal of the Society of* arc*hivists* 2006; 27: 213-226.
10. Padfield T, Larsen PK, Aasbjerg Jensen L and Ryhl-Svendsen, M. The potential and limits for passive air conditioning of museums, stores and archives. 2007.
11. Yang M, Kong F and He X. Moisture buffering effect of hygroscopic materials under wall moisture transfer. *Indoor and Built Environment* 2022; 31: 80-95.
12. Kukk V, Kers J, Kalamees T, Wang, L. and Ge, H. Impact of built-in moisture on the design of hygrothermally safe cross-laminated timber external walls: A stochastic approach. *Building and Environment* 2022; 226: 109736.
13. Padfield T, Ryhl-Svendsen M, Larsen PK and Aasbjerg Jensen, L. A review of the physics and the building science which underpins methods of low energy storage of museum and archive collections. *Studies in Conservation* 2018; 63: 209-215.
14. He Y, Han F, Zhao L and Li, S. Investigation of the indoor environment of a passive house office building under cold climate in China. *Indoor and Built Environment* 2022: 1420326X221126011.
15. Rahiminejad M and Khovalyg D. Numerical and experimental study of the dynamic thermal resistance of ventilated air-spaces behind passive and active façades. *Building and Environment* 2022; 225: 109616.
16. Yu M, Zhang X, Zhao Y and Zhang, X. A novel passive method for regulating both air temperature and relative humidity of the micro-environment in museum display cases. *Energies* 2019; 12: 3768.
17. Kumar S, Parida SS and Kumar N. Dehumidification performance improvement

by using liquid desiccant blends–An experimental study. *Indoor and Built Environment* 2023: 1420326X231151435.
18. Yang H, Peng Z, Zhou Y, Zhao, F., Zhang, J., Cao, X. and Hu, Z. Preparation and performances of a novel intelligent humidity control composite material. *Energy and buildings* 2011; 43: 386-392.
19. Stanley B, Xavier-Rowe A and Knight B. Displaying the wernher collection: A pragmatic approach to display cases. *The conservator* 2003; 27: 34-46.
20. Thickett D, Fletcher P, Calver A and Lambarth, S. The effect of air tightness on RH buffering and control. *Museum Microclimates* 2007: 245-251.
21. Chiantore O and Poli T. Indoor air quality in museum display cases: volatile emissions, materials contributions, impacts. *Atmosphere* 2021; 12: 364.
22. CONSERVATION K. Technical Knowledge No. 1 – Cotton or chemical wood pulp? No. 4 – Fillers, No. 6 "Polypropylene – A material for long-term archiving?", https://www.klug-conservation.com/Useful-knowledge (2022, accessed 28 February 2023).
23. dos Santos WN, Mummery P and Wallwork A. Thermal diffusivity of polymers by the laser flash technique. *Polymer testing* 2005; 24: 628-634.
24. Shinzato K and Baba T. A laser flash apparatus for thermal diffusivity and specific heat capacity measurements. *Journal of thermal analysis and calorimetry* 2001; 64: 413-422.
25. Golovin DY, Divin A, Samodurov A, Tyurin, A. I. and Golovin, Y. I. Determination of the Thermal Diffusivity of Materials by a Nondestructive Express Method with the Use of Step-By-Step Local Heating of the Surface and High-Speed Thermography. *Measurement Techniques* 2019; 62: 714-721.
26. ISO 13826:2013. Metallic and other inorganic coatings.
27. Slováčková B, Schmidtová J, Hrčka R and Mišíková, O. Diffusion Coefficient and Equilibrium Moisture Content of Different Wood Species Degraded with Trametes versicolor. *BioResources* 2021; 16.
28. BS EN ISO 12570:2000+A2:2018. Hygrothermal performance of building materials and products.
29. ISO E. 12571 Hygrothermal performance of building materials and products-Determination of hygroscopic sorption properties. *Brussels: European Committee for Standardization* 2013.
30. BS EN 15803:2009. Conservation of cultural property.
31. Schirmer R, ZVDI. *Beiheft Verfahrenstechnik*. 1938, p.170.
32. Testing ASf and Materials. *Standard test methods for water vapour transmission of materials*. ASTM International, 2013.
33. Crank J. *The mathematics of diffusion*. Oxford university press, 1979.
34. Zamel N, Li X and Shen J. Correlation for the effective gas diffusion coefficient in carbon paper diffusion media. *Energy & Fuels* 2009; 23: 6070-6078.
35. Ertekin T, King GR and Schwerer FC. Dynamic gas slippage: a unique dual-mechanism approach to the flow of gas in tight formations. *SPE formation evaluation* 1986; 1: 43-52.
36. Remion G, Moujalled B and El Mankibi M. Review of tracer gas-based methods

for the characterization of natural ventilation performance: Comparative analysis of their accuracy. *Building and Environment* 2019; 160: 106180.
37. ASTM E741-11. Standard Test Method for Determining Air Change in a Single Zone by Means of a Tracer Gas Dilution.
38. Grau-Bové J, Mazzei L, Strlic M and Cassar, M. Fluid simulations in heritage science. *Heritage Science* 2019; 7: 1-12.
39. Liu X, Song S, Tan Y, Fan, D., Ning, J., Li, X. and Yin, Y. Similar simulation study on the deformation and failure of surrounding rock of a large section chamber group under dynamic loading. *International Journal of Mining Science and Technology* 2021; 31: 495-505.
40. Camuffo D, Sturaro G and Valentino A. Showcases: a really effective mean for protecting artworks? *Thermochimica acta* 2000; 365: 65-77.
41. Bekesi J, Kaakkunen J, Michaeli W, Klaiber, F., Schoengart, M., Ihlemann, J. and Simon, P. Fast fabrication of super-hydrophobic surfaces on polypropylene by replication of short-pulse laser structured molds. *Applied Physics A* 2010; 99: 691-695.
42. Jose J, Thomas V, Raj A, John, J., Mathew, R. M., Vinod, V. and Mujeeb, A. Eco-friendly thermal insulation material from cellulose nanofibre. *Journal of Applied Polymer Science* 2020; 137: 48272.
43. Gane PA and Ridgway CJ. Moisture pickup in calcium carbonate coating structures: role of surface and pore structure geometry. *Nordic Pulp & Paper Rese*arch *Journal* 2009; 24: 298-308.
44. Derluyn H, Janssen H, Diepens J, Derome, D. and Carmeliet, J. Hygroscopic behavior of paper and books. *Journal of Building Physics* 2007; 31: 9-34.
45. Glaznev I, Alekseev V, Salnikova I, Elepov, B. and Aristov, Y. ARTIC-1: a new humidity buffer for showcases. *Studies in conservation* 2009; 54: 1-16.
46. Domínguez-Muñoz F, Anderson B, Cejudo-López JM and Carrillo-Andrés, A. Uncertainty in the thermal conductivity of insulation materials. *Energy and Buildings* 2010; 42: 2159-2168.
47. Fernández A, Martínez M, Segarra M, Martorell, I. and Cabeza, L. F. Selection of materials with potential in sensible thermal energy storage. *Solar energy materials and solar cells* 2010; 94: 1723-1729.
48. Sing KS. Reporting physisorption data for gas/solid systems with special reference to the determination of surface area and porosity (Recommendations 1984). *Pure and applied chemistry* 1985; 57: 603-619.
49. Haslach HW. The moisture and rate-dependent mechanical properties of paper: a review. *Mechanics of time-dependent materials* 2000; 4: 169-210.
50. Mendes N, Chhay M, Berger J and Dutykh, D. Numerical methods for diffusion phenomena in building physics. *PUCPress, Curitiba, Brazil* 2016; 1: 3.
51. Marrero TR and Mason EA. Gaseous diffusion coefficients. *Journal of Physical and Chemical Reference Data* 1972; 1: 3-118.
52. Watts S, Crombie D, Jones S and Yates, S. A. Museum showcases: specification and reality, costs and benefits. In: *Museum microclimates: contributions to the Copenhagen conference, 19-23 November 2007* 2007, pp.253-260.
53. Bacon L and Martin G. Out of Africa! Display case strategies—the theory and the

reality. *Studies in Conservation* 2000; 45: 18-23.
54. Thickett, David, and Sarah Allen. "Effect of temperature on off-gassing and corrosion." THE PROGRAMME (2018): 7.
55. Alvarez-Martin, Alba, and Gwénaëlle Kavich. "SPME-GC–MS for the off-gassing analysis of a complex museum object." Microchemical Journal 167 (2021): 106276.